

The Equation of State of the Unitary Fermi Gas: An Update on Lattice Calculations

Joaquín E. Drut¹, Timo A. Lähde², Gabriel Wlazłowski³, and Piotr Magierski^{3,4}

¹*Theoretical Division, Los Alamos National Laboratory, Los Alamos, NM 87545-0001, USA*

²*Helsinki Institute of Physics, P.O. Box 64, FI-00014 University of Helsinki, Finland*

³*Faculty of Physics, Warsaw University of Technology,
ulica Koszykowa 75, 00-662 Warsaw, Poland and*

⁴*Department of Physics, University of Washington, Seattle, Washington 98195-1560, USA*

(Dated: December 1, 2018)

The thermodynamic properties of the Unitary Fermi Gas (UFG) have recently been measured to unprecedented accuracy by Ku *et al.* at the MIT. In particular, these measurements provide an improved understanding of the regime below $T/\epsilon_F \simeq 0.20$, where a transition into a superfluid phase occurs. In light of this new development, we present an overview of state-of-the-art Auxiliary Field Quantum Monte Carlo (AFQMC) results for the UFG at finite temperature, comparing with the MIT data for the energy, chemical potential and density. These AFQMC results have been obtained using methods based on the Hybrid Monte Carlo (HMC) algorithm, which was first introduced within the context of Lattice QCD.

PACS numbers: 05.30.Fk, 03.75.Ss, 05.10.Ln

The Unitary Fermi Gas (UFG) is defined as a two-component many-fermion system in the limit of short interaction range r_0 and large s -wave scattering length a , such that $0 \leftarrow k_F r_0 \ll 1 \ll k_F a \rightarrow \infty$, with $k_F \equiv (3\pi^2 n)^{1/3}$ the Fermi momentum and n the particle number density (we shall choose units such that $\hbar = k_B = 1$). The UFG also saturates the unitarity bound on the quantum mechanical scattering cross section $\sigma_0(k) \leq 4\pi/k^2$, where k is the relative momentum of the colliding particles. The UFG features special properties that arise from the fact that it is characterized by a single length scale, given by the inter-particle distance $\sim k_F^{-1}$, independently of the details of the interaction. While the thermodynamic properties of the UFG are *universal* [1], the lack of a readily accessible dimensionless expansion parameter renders the UFG a challenging many-body problem. Since the proposal of the UFG as a model for dilute neutron matter by Bertsch [2] and its realization in ultracold atom experiments (see Ref. [3] for a review of the experimental situation), the UFG has received widespread attention, from atomic physics [4] to nuclear matter [5] and relativistic heavy-ion collisions [6].

On the experimental side, the presence of a superfluid phase in the UFG below $T/\epsilon_F \simeq 0.15$ was demonstrated directly a few years ago through the creation of an Abrikosov vortex lattice under rotation [7]. However, a direct thermodynamic signature of the transition was not unambiguously established until the recent high-precision measurement at the MIT of the Equation of State (EoS) of a homogeneous two-component UFG over a large temperature range [8]. These measurements were performed on trapped ⁶Li atoms (using a Feshbach resonance to tune the system to the unitary limit), which enabled a detailed study of the compressibility, density and pressure of the UFG. In addition, greatly refined empirical results were obtained for the associated critical temperature $T_c/\epsilon_F = 0.167(15)$, as well as for the “Bertsch pa-

rameter” $\xi = 0.376(5)$, which characterizes the ground state of the UFG. As precision data is now available for the energy, chemical potential and density of the UFG in a wide temperature range, an opportunity presents itself to compare these measurements with calculations in various theoretical frameworks. Here, we focus on comparing the MIT data with the most recent Auxiliary Field Quantum Monte Carlo (AFQMC) results.

The Hamiltonian that captures the physics of the unitary limit can be written on a spatial lattice as

$$\hat{H} \equiv \sum_{\mathbf{k}, \lambda=\uparrow, \downarrow} \frac{k^2}{2m} \hat{a}_\lambda^\dagger(\mathbf{k}) \hat{a}_\lambda(\mathbf{k}) - g \sum_i \hat{n}_\uparrow(\mathbf{r}_i) \hat{n}_\downarrow(\mathbf{r}_i), \quad (1)$$

where λ denotes the spin projection, m is the fermion mass (we also set $m = 1$), and g is the coupling constant. The creation and annihilation operators satisfy fermionic anticommutation relations, and $\hat{n}_\lambda(\mathbf{r}_i) \equiv \hat{a}_\lambda^\dagger(\mathbf{r}_i) \hat{a}_\lambda(\mathbf{r}_i)$ denotes the number density operator at lattice position \mathbf{r}_i for spin projection λ . The thermodynamic equilibrium properties are obtained from the grand canonical partition function

$$\mathcal{Z} \equiv \text{Tr} \exp[-\beta(\hat{H} - \mu\hat{N})], \quad (2)$$

where \hat{N} is the total particle number operator, μ denotes the chemical potential, and $\beta \equiv 1/k_B T$ is the inverse temperature.

To evaluate expectation values of observables numerically, we have followed the path integral approach presented extensively in Ref. [9], with recent further improvements described in Ref. [10]. The system is placed on a cubic spatial lattice of extent $L = N_x l$ with periodic boundary conditions. The lattice spacing l (henceforth set to unity) and extent L provide natural ultraviolet (UV) and infrared (IR) momentum cut-offs, given by $k_{\text{max}} = \pi/l$ and $k_0 = 2\pi/L$, respectively. The imaginary-time evolution operator $\exp[-\beta(\hat{H} - \mu\hat{N})]$ is expanded using a Trotter-Suzuki decomposition with temporal lattice

spacing τ , and the interaction is represented by means of a Hubbard-Stratonovich (HS) transformation [11]. As we focus on the spin-symmetric case, the fermion sign problem is absent. The resulting path integral formulation is an exact representation of Eq. (2) up to finite-volume and discretization effects, which may be controlled by varying the spatial lattice volume $V \equiv N_x^3$ and density n . The thermodynamic and continuum limits are recovered as $V \rightarrow \infty$ and $n \rightarrow 0$, respectively. The latter requires great care, as too low densities may introduce shell effects. As our lattice formulation is very similar to Ref. [9], we shall restrict ourselves to describing three modifications which significantly improve the results.

First, the value of the bare lattice coupling constant g corresponding to the unitary regime is determined by means of Lüscher’s formula [12] as in Ref. [13]. This procedure yields $g \simeq 5.14$ in the unitary limit. Our lattice Hamiltonian contains g as the sole parameter characterizing the interaction. As a consequence, finite-range effects are induced by the presence of the UV cutoff of the lattice. In order to minimize such discretization effects, the dilute limit should be approached as closely as possible. Recent theoretical developments [14] have explored the use of improved transfer matrices, with multiple parameters tuned to unitarity. The implementation of such methods is an objective of future AFQMC calculations.

Second, we use the compact, continuous HS transformation

$$\exp(\tau g \hat{n}_\uparrow(\mathbf{r}_i) \hat{n}_\downarrow(\mathbf{r}_i)) = \frac{1}{2\pi} \int_{-\pi}^{\pi} d\sigma_i [1 + B \sin(\sigma_i) \hat{n}_\uparrow(\mathbf{r}_i)] \times [1 + B \sin(\sigma_i) \hat{n}_\downarrow(\mathbf{r}_i)], \quad (3)$$

with σ_i the HS auxiliary field and $B^2/2 \equiv \exp(\tau g) - 1$. The above representation (referred to as “Type 4” in Ref. [15]) was found to be superior with respect to acceptance rate, decorrelation and signal-to-noise properties than the more conventional unbounded and discrete HS transformations [16]. In the context of AFQMC calculations of the Tan “contact” reported in Ref. [10], $\tau \simeq 0.05$ was found to be sufficiently small to render the Trotter-Suzuki error insignificant. However, for the EoS this matter is under further investigation, and forms one of the areas where future improvements to the AFQMC approach are expected.

Third, we update σ using Hybrid Monte Carlo (HMC), which combines the deterministic Molecular Dynamics (MD) evolution of σ with a Metropolis accept/reject step [17]. The applicability of the Determinantal Monte Carlo (DMC) algorithm (based on local Metropolis updates) is limited by the $\sim V^3$ scaling of the CPU time with the spatial lattice volume (although it should be noted that $\sim V^2$ scaling can be achieved using memory-intensive updating techniques [18]).

The net result is the Determinantal Hybrid Monte Carlo (DHMC) algorithm, introduced in Ref. [10]. In

DHMC, global MD updates of σ are implemented by means of a fictitious momentum field π which defines the DHMC Hamiltonian

$$\mathcal{H} \equiv \sum_i \frac{\pi_i^2}{2} - \log \det \left[(\mathbb{1} + \mathcal{U}[\sigma])^2 \right], \quad (4)$$

where $\mathcal{U}[\sigma]$ is a matrix which encodes the dynamics of the fermions (for more details on \mathcal{U} , see *e.g.* Ref. [9]). The DHMC algorithm produces greatly enhanced decorrelation between successive MC samples for all temperatures and lattice sizes, and removes the necessity to spend an increasing number of decorrelation steps at larger V (note that the computational cost of a full sweep of the lattice scales as $\sim V$ in a local algorithm such as DMC). This is replaced by a fixed number of operations, typically of $\mathcal{O}(10^2)$, required to produce one MD “trajectory”, independently of V .

The scaling properties of DHMC are somewhat involved to estimate, as the CPU time taken by merely forming the matrix $\mathcal{U}[\sigma]$, given a configuration of σ , typically greatly exceeds the time taken by any subsequent operations on that matrix. Examples include the evaluation of $\det(\mathbb{1} + \mathcal{U}[\sigma])$ in DMC and the computation of \mathcal{U}^{-1} , which appears in the “force” governing the MD evolution in DHMC. While the evaluation of the inverse scales as $\sim V^3$, it is independent of N_τ . On the other hand, forming the elements of $\mathcal{U}[\sigma]$ scales as $\sim N_\tau \times V^2 \log V$. This dependence arises from evolving, in N_τ steps, a basis set of V single-particle wave functions using a fast Fourier transform (FFT), which scales roughly as $\sim V \log V$ per wave function. Thus, for fixed N_τ , the CPU time consumed by DHMC effectively scales as

$$t_{\text{DHMC}} = AV^3 + BV^2 \log V, \quad (5)$$

with the spatial lattice volume V , where $A \ll B$. For N_x up to $\sim 14 - 16$, we find that the scaling of the DHMC algorithm (in its simplest implementation) closely follows the $\sim V^2 \log V$ law, at which point excessive memory requirements become a limiting factor for current desktop systems, as DHMC is not a “matrix-free” method. The maximum N_x to which DHMC is feasible depends on the availability of memory as well as the degree of sophistication of the implementation. Maintaining the relationship $A \ll B$ is an active area of development, with favorable scaling currently possible beyond $N_x \simeq 20$.

The DHMC algorithm has allowed us to extend the AFQMC analysis of the EoS beyond the capabilities of the DMC approach, which is currently limited to $N_x \simeq 10$ in the spatial lattice extent, $n \approx 0.1$ in the particle number density, and $N \approx 100$ in the particle number. The improved scaling of the CPU time has allowed us to study lattices as large as $N_x = 14$ with $n \approx 0.04$, while simultaneously maintaining a relatively large number of particles, $N \approx 45, 75$ and 110 for $N_x = 10, 12$ and 14 , respectively. For each T/ϵ_F , we have generated $\simeq 200$

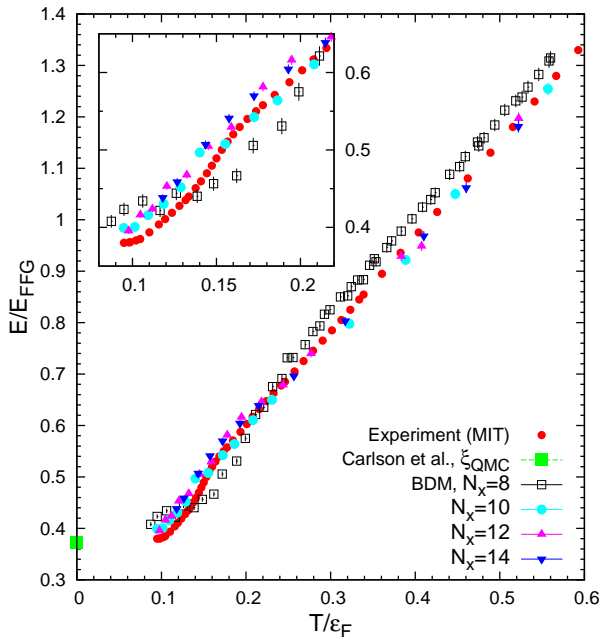


FIG. 1: (Color online) Energy E/E_{FFG} (red dots), in units of the energy of a free Fermi gas $E_{\text{FFG}} = 3/5 N \epsilon_F$, as obtained by Ku *et al.* [8]. Our AFQMC results using the DHMC algorithm (with $\tau = 0.05$) are shown for different spatial lattice volumes $V \equiv N_x^3$, for $N_x = 14$ (blue triangles), for $N_x = 12$ (purple triangles) and $N_x = 10$ (light blue dots). The results for $N_x = 8$ (open black squares) were obtained with the DMC algorithm in Ref. [9]. The inset shows the low-temperature region around the critical temperature $T_c/\epsilon_F \simeq 0.15$ of the superfluid phase transition. The green square shows the QMC result of Ref. [19] for ξ at $T = 0$.

uncorrelated snapshots of σ which yields a statistical uncertainty of $\simeq 1\%$ for the observables considered here. Our DHMC results can then be contrasted with the experimental data of the MIT group [8], to assess the accuracy of current AFQMC techniques.

In Fig. 1, we show a comparison between AFQMC results and the measured energy E of the homogeneous UFG. The overall agreement with experiment is satisfactory throughout the range of temperatures studied. In the low-temperature region, DHMC slightly overpredicts the experimental data. Our new results represent a noticeable improvement over DMC calculations [9] with $N_x = 8$, likely due to decreased finite volume and residual effective range effects. In Fig. 2, we present a similar analysis for the chemical potential μ/ϵ_F . In contrast to the case of E , the DHMC results for μ/ϵ_F clearly deviate from experiment at low T/ϵ_F , which indicates $\mu/\epsilon_F \simeq 0.38$ at $T/\epsilon_F \simeq 0.1$. DHMC overestimates this by $\simeq 5\%$, which clearly exceeds the statistical uncertainty. However, it should be noted that our larger lattices represent a dramatic improvement over the $N_x = 8$ description of μ/ϵ_F , in particular above $T_c/\epsilon_F \simeq 0.15$. Still, the discrepancy below T_c/ϵ_F clearly calls for further study and

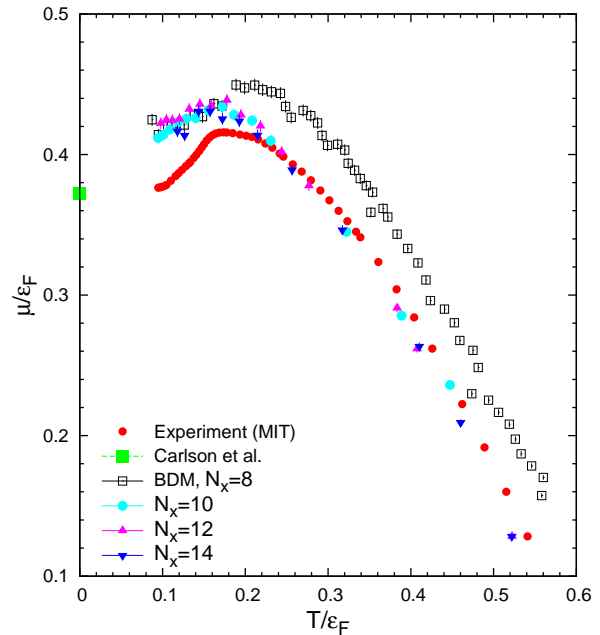


FIG. 2: (Color online) Chemical potential μ in units of the Fermi energy ϵ_F as measured by Ku *et al.* [8]. The notation for the AFQMC results is identical to Fig. 1. The green square shows the result of Ref. [19] assuming $\mu/\epsilon_F(T = 0) = \xi$.

improvements to the AFQMC framework. In Fig. 3, we present our DHMC results for the particle number density, relative to the temperature-dependent density of the non-interacting Fermi gas. Again, a discrepancy at low temperatures is observed, which is clearly similar to the effects observed for μ/ϵ_F .

While the agreement between our AFQMC calculation and the data of Ref. [8] is satisfactory in general, notable discrepancies persist. The present DHMC studies have achieved a significant reduction of the density from $n \simeq 0.1$ to $n \simeq 0.04$ with a concomitant reduction in discretization (finite density) effects. The DHMC calculation of the Tan contact in Ref. [10] showed that such effects are largest for high T/ϵ_F . Moreover, preliminary indications were found that a density of $n \simeq 0.03 - 0.04$ is sufficiently low to render the finite density effects insignificant for $T/\epsilon_F \leq 0.25$. While such conclusions may be strongly dependent on the observable under consideration, we note that the $N_x = 8$ DMC data of Ref. [9] agree closely with our DHMC data for $T/\epsilon_F \leq 0.20$. While this may indicate that finite density effects are small at low T/ϵ_F , a thorough investigation is clearly called for. A systematic improvement of the Hamiltonian in the spirit of Ref. [14] may provide a practical way to remove residual finite-range effects. Another possible effect is the Trotter-Suzuki error, although it was found to be small in Ref. [10]. An effort is underway to obtain DHMC data for smaller τ . In spite of these shortcomings, the introduction of HMC into the AFQMC study of the UFG has largely solved the issue of sufficiently large spatial lattice

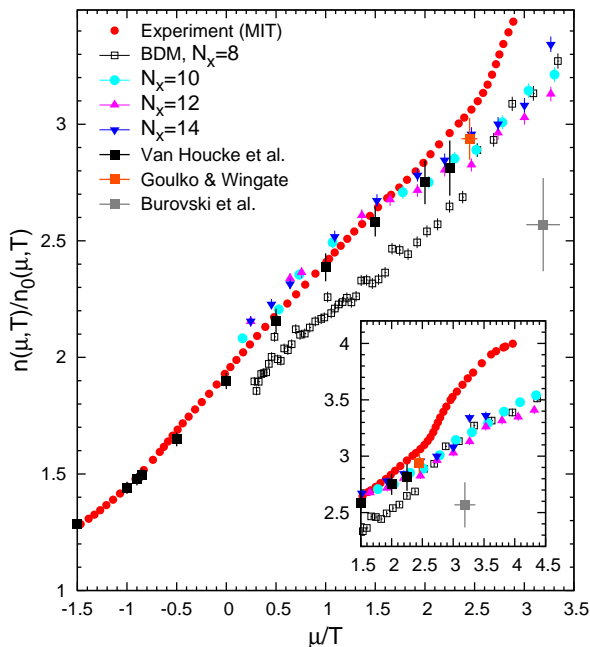


FIG. 3: (Color online) Density $n(\mu, T)$ of the UFG (red circles) as obtained by Ku *et al.* [8], normalized to the density $n_0(\mu, T)$ of a non-interacting Fermi gas. The notation for the AFQMC results is identical to Fig. 1. The Diagrammatic MC results of Refs. [20, 21] and the BDMC results of Ref. [22] are shown as well (filled squares). The inset shows the region at low T/ϵ_F where the deviation from experiment is largest.

dimension N_x and particle number N , which in turn has allowed calculations with a large particle number at low densities. DHMC studies for $N_x > 14$ are in progress.

The recent Bold Diagrammatic Monte Carlo (BDMC) results of Ref. [22] exhibit a level of agreement with the data of Ref. [8] comparable to our DHMC results in the region above T_c . Intriguingly, Fig. 3 suggests that the BDMC and DHMC results deviate similarly from the experimental data as T_c is approached from above. Both approaches may thus be plagued by the same hitherto unidentified effect, which gives rise to an increasing deviation from experiment at low T/ϵ_F .

Acknowledgments

We thank M. Zwierlein for making the data of the MIT experiment available to us, and F. Werner for providing us with the most recent BDMC results. We are indebted to A. Bulgac for instructive discussions and a careful reading of the manuscript. We acknowledge support under U.S. DOE Grant DE-FC02-07ER41457, and contract N N202 128439 of the Polish Ministry of Science. This study was supported, in part, by the Vilho, Yrjö, and Kalle Väisälä Foundation of the Finnish Academy of Science and Letters, and by the Magnus Ehrnrooth, the Waldemar von Frenckell and the Nils-Erik and Ruth Stenbäck Foundations of the Finnish Society of Sciences

and Letters. One of the authors (G.W.) acknowledges the Polish Ministry of Science for the support within the program “Mobility Plus - I edition” under contract No. 628/MOB/2011/0. Some calculations were performed at the Interdisciplinary Centre for Mathematical and Computational Modelling (ICM) at Warsaw University.

-
- [1] H. Heiselberg, Phys. Rev. A **63**, 043606 (2001); T.-L. Ho, Phys. Rev. Lett. **92**, 090402 (2004).
 - [2] “The Many-Body Challenge Problem”, formulated by G. F. Bertsch (1999), see *e.g. Series on Advances in Quantum Many-Body Theory - Vol. 3*, R. F. Bishop, K. A. Gernoth, N. R. Walet, Y. Xian (Eds.) (World Scientific, Singapore, 2000).
 - [3] *Ultracold Fermi Gases*, Proceedings of the International School of Physics “Enrico Fermi”, Course CLXIV, Varenna, June 20 – 30, 2006, M. Inguscio, W. Ketterle, C. Salomon (Eds.) (IOS Press, Amsterdam, 2008).
 - [4] S. Giorgini, L. P. Pitaevskii, S. Stringari, Rev. Mod. Phys. **80** (2008) 1215; I. Bloch, J. Dalibard, W. Zwerger, *ibid.* **80** (2008) 885.
 - [5] C. J. Pethick, D. G. Ravenhall, Ann. Rev. Nucl. Part. Science **45**, 429 (1995); J. Carlson *et al.*, Phys. Rev. C **68**, 025802 (2003); C. J. Horowitz, A. Schwenk, Phys. Lett. B **638** 153 (2006). A. Gezerlis, J. Carlson, Phys. Rev. C **77**, 032801(R) (2008).
 - [6] T. Schäfer, Physics **2**, 88 (2009); T. Schäfer, D. Teaney, Rept. Prog. Phys. **72**, 126001 (2009).
 - [7] M. W. Zwierlein *et al.* Nature **435**, 1047 (2005).
 - [8] M. J. H. Ku, A. T. Sommer, L. W. Cheuk, M. W. Zwierlein, arXiv:1110.3309.
 - [9] A. Bulgac, J. E. Drut, P. Magierski, Phys. Rev. Lett. **96**, 090404 (2006); Phys. Rev. A **78**, 023625 (2008); A. Bulgac, M. M. Forbes, P. Magierski, in *BCS-BEC Crossover and the Unitary Fermi Gas* (Chap. 9), W. Zwerger (Ed.) (Springer, Berlin, 2011), *to be published*.
 - [10] J. E. Drut, T. A. Lähde, T. Ten, Phys. Rev. Lett. **106**, 205302 (2011).
 - [11] R. L. Stratonovich, Sov. Phys. Dokl. **2**, 416 (1958); J. Hubbard, Phys. Rev. Lett. **3**, 77 (1959).
 - [12] M. Lüscher, Commun. Math. Phys. **105**, 153 (1986).
 - [13] D. Lee, T. Schäfer, Phys. Rev. C **73**, 015201 (2006); Phys. Rev. C **73**, 015202 (2006).
 - [14] M. G. Endres, D. B. Kaplan, J.-W. Lee, A. N. Nicholson, arXiv:1106.5725; arXiv:1106.0073; PoS **LAT2010**, 182 (2010); J.-W. Lee, M. G. Endres, D. B. Kaplan, A. N. Nicholson, arXiv:1011.3026, PoS **LAT2010**, 197 (2010), A. N. Nicholson, M. G. Endres, D. B. Kaplan, J.-W. Lee, arXiv:1011.2804; PoS **LAT2010**, 206 (2010).
 - [15] D. Lee, Phys. Rev. C **78**, 024001 (2008); Prog. Part. Nucl. Phys. **63**, 117 (2009).
 - [16] J. E. Hirsch, Phys. Rev. B **28**, 4059(R) (1983).
 - [17] S. Duane *et al.*, Phys. Lett. B **195**, 216 (1987); S. A. Gottlieb *et al.*, Phys. Rev. D **35**, 2531 (1987).
 - [18] R. R. dos Santos, Braz. J. Phys. **33**, 36 (2003).
 - [19] J. Carlson *et al.*, arXiv:1107.5848.
 - [20] E. Burovski, N. Prokof’ev, B. Svistunov, M. Troyer, Phys. Rev. Lett. **96**, 160402 (2006).
 - [21] O. Goulko, M. Wingate, Phys. Rev. A **82**, 053621 (2010).
 - [22] K. Van Houcke *et al.*, arXiv:1110.3747.